DISEASES AND DISORDERS

Fentanyl vapor self-administration model in mice to study opioid addiction

K. Moussawi[1,2*†], M. M. Ortiz[1†], S. C. Gantz[1,3], B. J. Tunstall[1], R. C. N. Marchette[1], A. Bonci[4], G. F. Koob[1], L. F. Vendruscolo[1*]

Intravenous drug self-administration is considered the "gold standard" model to investigate the neurobiology of drug addiction in rodents. However, its use in mice is limited by frequent complications of intravenous catheterization. Given the many advantages of using mice in biomedical research, we developed a noninvasive mouse model of opioid self-administration using vaporized fentanyl. Mice readily self-administered fentanyl vapor, titrated their drug intake, and exhibited addiction-like behaviors, including escalation of drug intake, somatic signs of withdrawal, drug intake despite punishment, and reinstatement of drug seeking. Electrophysiological recordings from ventral tegmental area dopamine neurons showed a lower amplitude of $GABA_B$ receptor–dependent currents during protracted abstinence from fentanyl vapor self-administration. This mouse model of fentanyl self-administration recapitulates key features of opioid addiction, overcomes limitations of the intravenous model, and allows investigation of the neurobiology of opioid addiction in unprecedented ways.

INTRODUCTION

Opioid use disorder is a major worldwide public health concern (*1*). Its prevalence and associated mortality are escalating globally (*1*, *2*), and opioid overdose deaths have reached epidemic proportions (*3*). Fentanyl, a synthetic opioid that is commonly used clinically for anesthesia and analgesia, accounts for nearly 46% of opioid overdose deaths (*3*). It is commonly administered intravenously or by inhalation (smoking/vaping), resulting in rapid drug bioavailability in the brain (*4*).

Currently, intravenous self-administration models are the "gold standard" to study opioid addiction in rodents (*5*). Rat models of intravenous opioid self-administration and relapse are widely used and have been instrumental in understanding brain circuits that control drug taking and seeking and drug-induced neuroadaptations (*6*, *7*). However, despite major advances in preclinical opioid addiction research, large knowledge gaps in understanding the unique aspects of opioid addiction persist.

Mouse models offer unique advantages compared with rats in neurobiological investigations when considering the numerous behaviorally selected and transgenic mouse strains that allow genetic targeting and manipulation using sophisticated techniques (e.g., imaging, chemogenetics, and optogenetics). Although intravenous self-administration models in mice have been used successfully (*8*, *9*), the use of such models in opioid addiction research remains very scarce and restricts the duration of exposure to drugs because of high catheter failure rates, especially during prolonged access to drugs (*8*, *10*). Intravenous catheters also limit the ability to perform in vivo electrophysiology or calcium imaging experiments in freely moving mice, in part, because of double tethering.

Given the similarities in pharmacokinetics and pharmacodynamics of inhaled and intravenously infused drugs (*11*), we developed and validated a noninvasive mouse model to study the neurobiology of opioid addiction using vaporized fentanyl, which overcomes many limitations of intravenous models. Mice exhibited several somatic and motivational signs of opioid dependence that resembled opioid use disorder in humans. We also identified long-lasting γ-aminobutyric acid (GABA)ergic neuroadaptations in ventral tegmental area (VTA) dopamine neurons after protracted abstinence.

RESULTS

Vaporized fentanyl-induced analgesia

We first determined a concentration-response function for the analgesic effects of vaporized fentanyl using the hot-plate test. Different concentrations of fentanyl (0 to 30 mg/ml) were vaporized using a modified e-cigarette device (fig. S1). Mice (n = 8 to 24 males) were placed in the behavior chambers and passively exposed to vaporized fentanyl. One minute after the last fentanyl vapor delivery, the mice were placed on a hot plate, and the latency to signs of nociception was recorded. Vaporized fentanyl dose-dependently increased nociception latency, whereas vehicle vapor in the absence of drug had no effect (Fig. 1A).

Vaporized fentanyl-induced locomotion

On the basis of the concentration-dependent analgesic effects of fentanyl, we investigated the effects of vaporized fentanyl (2.5, 5, and 10 mg/ml) on locomotor activity, a function of the fentanyl effects on the mesolimbic dopaminergic system (*12*). A separate cohort of mice (n = 34, F/M = 18/16) was placed in locomotor activity boxes for 30 min to measure baseline locomotion. The mice were then passively exposed to vaporized fentanyl. One minute after the last fentanyl vapor delivery, the mice were returned to the locomotor activity boxes. Fentanyl significantly increased locomotor activity in a concentration-dependent manner (Fig. 1B).

Blood fentanyl levels

To confirm that exposure to different concentrations of vaporized fentanyl correlates with blood fentanyl levels, drug-naïve mice were passively exposed to fentanyl vapor (five vapor deliveries over 1 hour) at 2.5 mg/ml (n = 9, F/M = 4/5) or 10 mg/ml (n = 10, F/M = 5/5).

[1]Intramural Research Program, National Institute on Drug Abuse, National Institutes of Health, Baltimore, MD, USA. [2]Neurology Department, Johns Hopkins Medicine, Baltimore, MD, USA. [3]Department of Molecular Physiology and Biophysics, University of Iowa, Iowa City, IA, USA. [4]Global Institutes on Addictions, Miami, FL, USA.
*Corresponding author. Email: moussawi.khaled@gmail.com (K.M.); leandro.vendruscolo@nih.gov (L.F.V.)
†These authors contributed equally to this work.

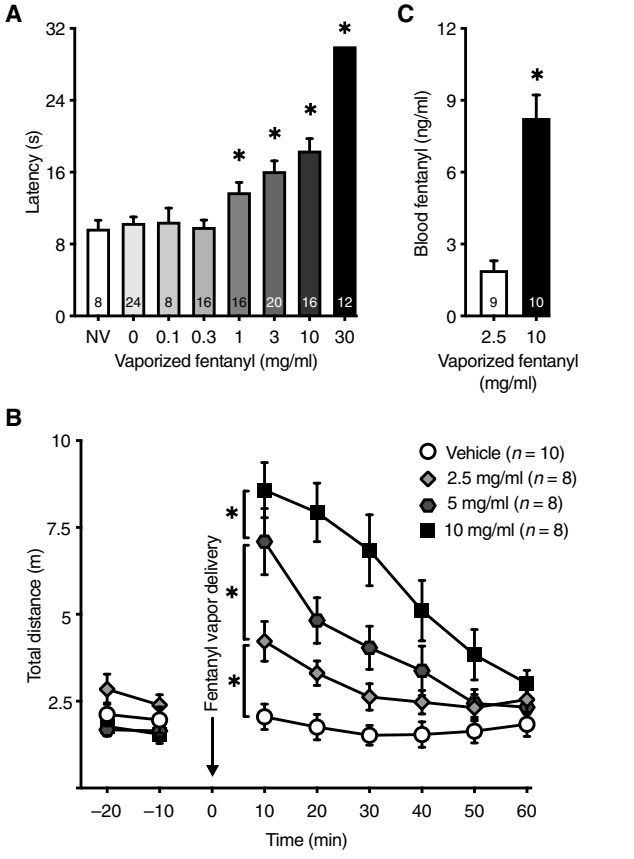

Fig. 1. Vaporized fentanyl induces analgesia and increases locomotor activity. (**A**) Passive administration of vaporized fentanyl (four vapor deliveries over 8 min) increased the latency to nociception in the hot-plate test [one-way analysis of variance (ANOVA); $F_{7,112} = 38.45$; $P < 0.0001$] in a concentration-dependent manner. Sidak's multiple comparisons test shows that the 1, 3, 10, and 30 mg/ml groups were significantly different from vehicle. "NV" indicates mice that were not exposed to fentanyl or vehicle vapor. (**B**) Locomotor activity in meters was measured at baseline and after passive exposure to different concentrations of vaporized fentanyl (five vapor deliveries over 10 min) versus vehicle vapor (0 mg/ml). Locomotor activity increased with the concentration of vaporized fentanyl [two-way repeated-measures (RM) ANOVA; concentration × time interaction $F_{15,150} = 10.14$; $P < 0.0001$]. Sidak's multiple comparisons test shows significant differences in locomotion between the different concentrations. (**C**) Blood fentanyl levels in response to five fentanyl vapor deliveries (2.5 mg/ml: 1.91 ± 0.39 ng/ml; 10 mg/ml: 8.27 ± 0.95 ng/ml) that were passively delivered over 1 hour (unpaired *t* test; $t_{17} = 5.93$; $P < 0.0001$). The ratio of fentanyl blood levels at 10 and 2.5 mg/ml (8.27/1.91 = 4.3) is a close approximation of the ratio of fentanyl concentrations (10/2.5 = 4). The regression analysis of measured blood fentanyl levels yields a slope $a = 0.85$ (CI: 0.55 to 1.15; $F_{1,17} = 35.14$; $r^2 = 0.67$; $P < 0.0001$), which is not different from the presumed linear metabolism slope ($a = \frac{(1.91 \times 4) - 1.91}{10 - 2.5} = 0.76$; test of equal slopes $F_{1,17} = 0.033$; $P = 0.86$), suggesting that fentanyl metabolism was linear within the range of five vapor deliveries over 1 hour at 2.5 and 10 mg/ml, equivalent to a range of 12.5 to 50 mg/ml per hour. The number of mice (*n*) is shown in the graphs. The data are expressed as means ± SEM. *$P < 0.05$.

Blood samples were collected 2 min after the last vapor delivery. Blood fentanyl levels were significantly higher after vaporized fentanyl at 10 mg/ml compared with 2.5 mg/ml and reflected the linear metabolism of fentanyl within the experimental range of fentanyl concentrations and number of vapor deliveries (Fig. 1C). Blood fentanyl levels were higher in females than in males in response to fentanyl (10 mg/ml) (fig. S2A). This difference may be attributable to the lower body weight of females (females, 19.6 ± 0.7 g; males, 28.2 ±1.3 g; $t_8 = 5.9$, $P = 0.0004$), which was supported by a negative correlation between body weight and blood fentanyl levels at 10 mg/ml (fig. S2B). Another possibility is that fentanyl is metabolized more slowly in females than in males. An intraperitoneal injection of 0.2 mg/kg fentanyl, a dose that was previously reported to induce analgesia, conditioned hyperlocomotion, and conditioned place preference in mice (*13*), resulted in comparable blood fentanyl levels and locomotor activity to vaporized fentanyl (2.5 mg/ml) (fig. S2, C and D).

Fentanyl vapor self-administration at different fentanyl concentrations

Using a fixed-ratio 1 (FR1) schedule of reinforcement, a separate group of mice ($n = 16$ males) quickly learned to nosepoke for fentanyl vapor in 1-hour sessions (movie S1). The mice initially self-administered vaporized fentanyl (10 mg/ml) for eight sessions, followed by eight sessions at 5 mg/ml and then eight sessions at 2.5 mg/ml (Fig. 2A). This experiment was conducted with two groups of mice ($n = 8$ per group) under different vaporizer power settings that were adjusted to allow exposure to fentanyl vapor for ~1 min (60 W for 1.5 s versus 20 W for 5 s). The data were pooled because both groups exhibited similar results. Mice titrated their fentanyl vapor self-administration based on the fentanyl concentration (i.e., increased active responding with a lower fentanyl concentration) (Fig. 2, A and B). Inactive nosepokes were not different at the different fentanyl concentrations, and the number of active nosepokes was higher than the number of inactive nosepokes, indicating clear discrimination between the two nosepoke ports (Fig. 2B).

To estimate blood fentanyl levels after the self-administration of different fentanyl concentrations, we used data from Fig. 1C to generate a regression equation ($y = 0.6231x$). These data reflect blood fentanyl levels after five vapor deliveries that were passively delivered over 1 hour. We calculated the average blood fentanyl level for each vapor delivery at 10, 5, and 2.5 mg/ml ($y/5$), multiplied by the average number of vapor deliveries at each fentanyl concentration (data from Fig. 2A). The results showed equivalent blood fentanyl levels after vapor self-administration at different fentanyl concentrations (fig. S3A), again indicating that the mice titrated their drug self-administration to their preferred levels.

We also tested the self-administration of vaporized fentanyl at 1 mg/ml in a separate cohort of mice ($n = 12$ males). The mice did not maintain a stable level of fentanyl vapor self-administration at this concentration (fig. S3, B and C). Although the 2.5 mg/ml concentration elicited a peak self-administration response relative to 10, 5, and 1 mg/ml, the variability in the number of active nosepokes and vapor deliveries at 2.5 mg/ml was higher than at 10 and 5 mg/ml, as measured by the coefficient of variation that was averaged across sessions and animals at each concentration. The coefficient of variation at 10, 5, 2.5, and 1 mg/ml was 16.0, 16.6, 41.0, and 30.3% for active nosepokes, 16.0, 17.8, 22.6, and 27.1% for vapor deliveries, and 25.1, 28.5, 24.4, and 27.2% for inactive nosepokes, respectively. Therefore, we chose the 5 mg/ml fentanyl concentration for the subsequent experiments.

Fentanyl vapor self-administration under different schedules of reinforcement

To test whether mice would expend more effort ("cost") to obtain fentanyl, a separate cohort of mice was tested for fentanyl vapor

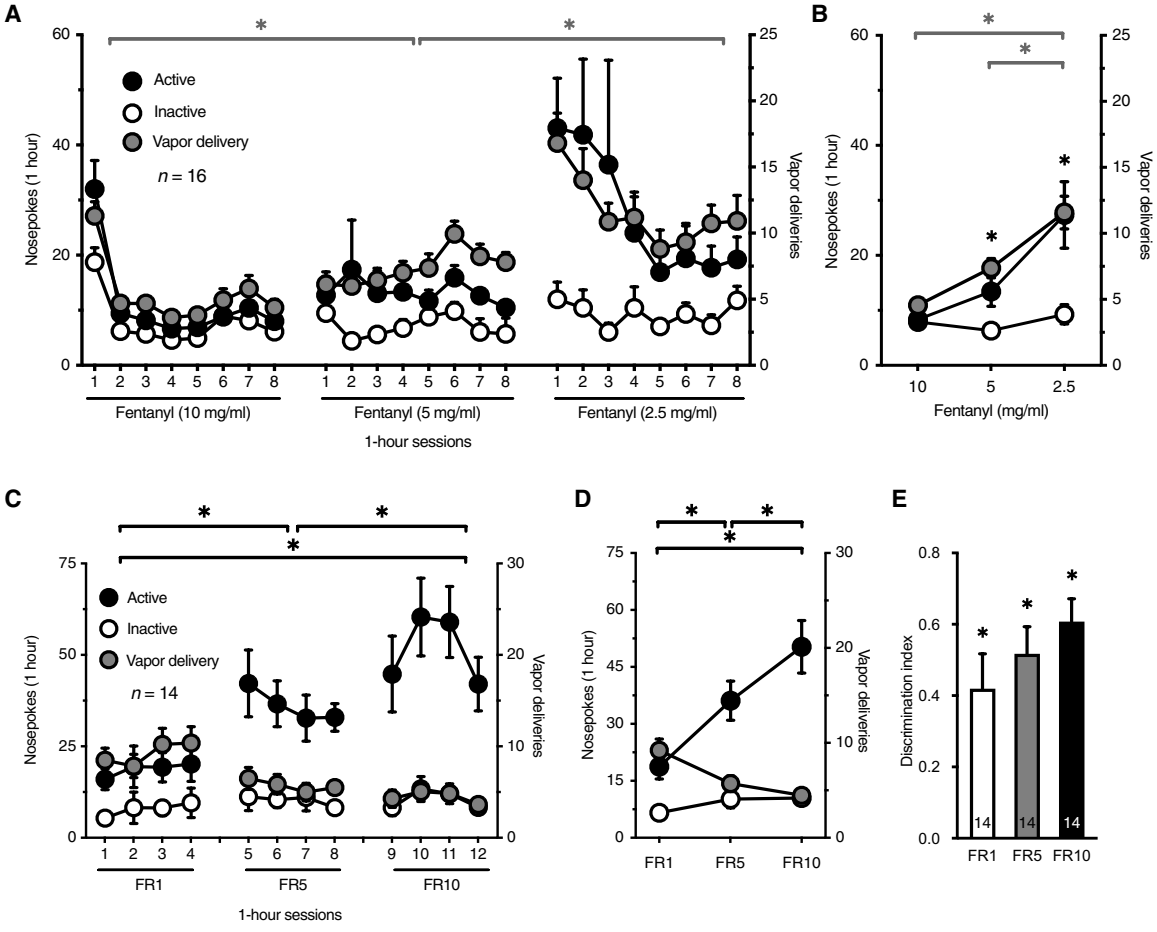

Fig. 2. Mice self-administer fentanyl vapor and titrate their intake in response to different vaporized fentanyl concentrations and reinforcement schedules. (**A**) Mice self-administered fentanyl vapor in 1-hour sessions on an FR1 schedule and increased their responding when the concentration of vaporized fentanyl was reduced from 10 to 5 to 2.5 mg/ml. The graph shows the number of active and inactive nosepokes (NP) (left *y* axis) and vapor deliveries (VD) (right *y* axis) in each self-administration session. Two-way RM ANOVA shows a significant concentration × session interaction ($F_{3.73,55.98} = 4.26$; $P = 0.005$) and significant effect of concentration on the number of VD ($F_{1.38,20.65} = 23.84$; $P < 0.0001$). A similar analysis shows a significant effect of fentanyl concentration on the number of active NP ($F_{1.15,17.21} = 9.73$; $P = 0.005$). The number of inactive NP did not change ($P = 0.38$). (**B**) Average of all self-administration sessions at each concentration (the first session at 10 mg/ml was a significant outlier per Grubbs' test likely because of a novelty effect and was not included in the data analyses). Mice discriminated between active and inactive NP operandum as the fentanyl concentration changed. Two-way RM ANOVA shows a significant concentration × NP interaction ($F_{1.16,17.39} = 10.88$; $P = 0.003$). (**C**) Mice exhibited an increase in the number of active NP when they were switched from an FR1 to FR5 schedule and then to an FR10 schedule (two-way RM ANOVA; $F_{1.48,19.20} = 19.20$; $P = 0.0002$). The number of inactive NP did not change. The number of VD decreased with increasing FR (two-way RM ANOVA; $F_{1.27,16.51} = 16.35$; $P = 0.0005$). (**D**) Averaged data from (C) at each FR. (**E**) The discrimination index of fentanyl vapor self-administration was greater than 0 for FR1, FR5, and FR10 (one-sample *t* test; FR1: $t_{13} = 4.28$, $P = 0.0009$; FR5: $t_{13} = 6.82$, $P < 0.0001$; FR10: $t_{13} = 9.50$, $P < 0.0001$). The discrimination index increased with increasing FR schedule (one-way RM ANOVA; $F_{1.65,21.39} = 4.17$; $P = 0.036$). The number of mice (*n*) is shown in the graphs. The data are expressed as means ± SEM. *$P < 0.05$.

self-administration under different schedules of reinforcement. Mice (n = 14, F/M = 6/8) self-administered fentanyl vapor (5 mg/ml) on an FR1 schedule in four sessions, followed by four sessions on an FR5 schedule and four sessions on an FR10 schedule. The mice exhibited a significant increase in the number of active nosepokes at higher FR schedules (Fig. 2, C and D). The number of inactive nosepokes did not change with FR schedule. Although the number of vapor deliveries was lower at higher FR schedules, the discrimination index ([active nosepokes − inactive nosepokes]/[active nosepokes + inactive nosepokes]) was significantly greater than 0 for all FR schedules and increased at higher FR schedules, thus reflecting the specificity of active nosepoke responses (Fig. 2E).

A cohort of mice (n = 14, F/M = 7/7) that self-administered vehicle vapor in the absence of fentanyl did not increase their active nosepoke responding when the reinforcement schedule was increased from FR1 to FR5 and FR10, and the number of vapor deliveries decreased significantly at higher FRs (fig. S4, A and B). Similarly, a separate cohort of mice (n = 8, F/M = 4/4) responded for the light cue in the absence of vehicle or fentanyl vapor, but the number of nosepokes did not change with FR, and the number of light cue presentations decreased significantly at higher FRs (fig. S4, C and D).

When the data were normalized, the relative increase in the number of active nosepokes between FR10 and FR1 was significantly greater in the fentanyl vapor group than in the vehicle vapor and light cue groups (fig. S4E). The relative decrease in the number of vapor deliveries between FR10 and FR1 was significantly smaller in the fentanyl vapor group than in the vehicle vapor and light cue

groups (fig. S4F). Furthermore, the discrimination index at FR1 was significantly larger in the fentanyl vapor group than in the vehicle vapor group (fig. S4G). These data indicate that fentanyl vapor was more reinforcing than vehicle vapor or the light cue.

Extinction and reinstatement of fentanyl vapor self-administration

We used a paradigm of extinction followed by cue-induced reinstatement to model relapse. A separate cohort of mice ($n = 7$ males) self-administered fentanyl vapor (5 mg/ml) in eight 1-hour sessions (FR1), in which vapor deliveries were associated with light cue presentation. On day 9, the mice began extinction training in the absence of cues, during which they were placed in the vapor chambers in 1-hour sessions, but both active and inactive nosepoke responses had no scheduled consequences (Fig. 3A). The number of active nosepokes significantly increased on day 1 of extinction, reflecting drug seeking (Fig. 3B). The mice continued extinction training for 30 sessions, during which the number of active nosepokes significantly decreased, demonstrating the extinction of drug seeking (Fig. 3A). The number of active nosepokes at the end of extinction training remained higher than during the self-administration sessions, an effect that was previously observed in rats (*14*). This is likely because nosepoking is a prepotent response in rodents that was suppressed during fentanyl self-administration because of fentanyl's pharmacological effect but was unfettered in the absence of fentanyl.

After the last day of extinction, we tested the light cue–induced reinstatement of drug seeking. During the reinstatement session (1 hour), the light cue was presented the same way as during the previous self-administration sessions (1-min duration in response to active nosepoke). The results indicated that the light cue significantly reinstated drug seeking (Fig. 3C).

In the next experiment, we tested whether mice extinguish fentanyl vapor self-administration when vehicle vapor and the light cue are available during extinction sessions. A subgroup ($n = 8$) of the cohort that underwent FR1-FR5-FR10 testing (from Fig. 2C) was transitioned to extinction after their last FR10 self-administration session. These sessions were essentially FR10 vehicle vapor self-administration sessions. The mice did not extinguish nosepoke responses for vehicle vapor and the light cue over 30 sessions (fig. S5A), but the number of active nosepokes was similar to the vehicle vapor self-administration experiment in mice that were never exposed to fentanyl (fig. S4, A and B). The maintenance of active nosepoke responding during extinction in the presence of vehicle vapor and the light cue could be attributed to one or more of the following: (i) vehicle vapor and the light cue that were previously conditioned to fentanyl delivery serve as powerful conditioned reinforcers (*15*, *16*), (ii) vehicle vapor has a sweet flavor because of glycerol and may be reinforcing, and (iii) nosepoking is a prepotent response in rodents. Thus, when designing extinction studies, one needs to consider prepotent responding on the operandum (e.g., nosepoke versus lever press) and possible intrinsic reinforcing properties of the cues or the vehicle that is used to dissolve and vaporize the drug of interest (e.g., appetitive sensory properties).

Escalation of fentanyl vapor self-administration

To test whether mice develop tolerance and escalate fentanyl vapor self-administration, three cohorts of mice were trained as follows: (i) short-access fentanyl (ShA-Fen) group ($n = 16$, F/M = 8/8) that self-administered fentanyl vapor in 1-hour sessions throughout the experiment; (ii) long-access vehicle (LgA-Veh) group ($n = 12$, F/M = 8/4) that self-administered vehicle vapor in 1-hour sessions (eight sessions), followed by 12-hour sessions (10 sessions, every other day);

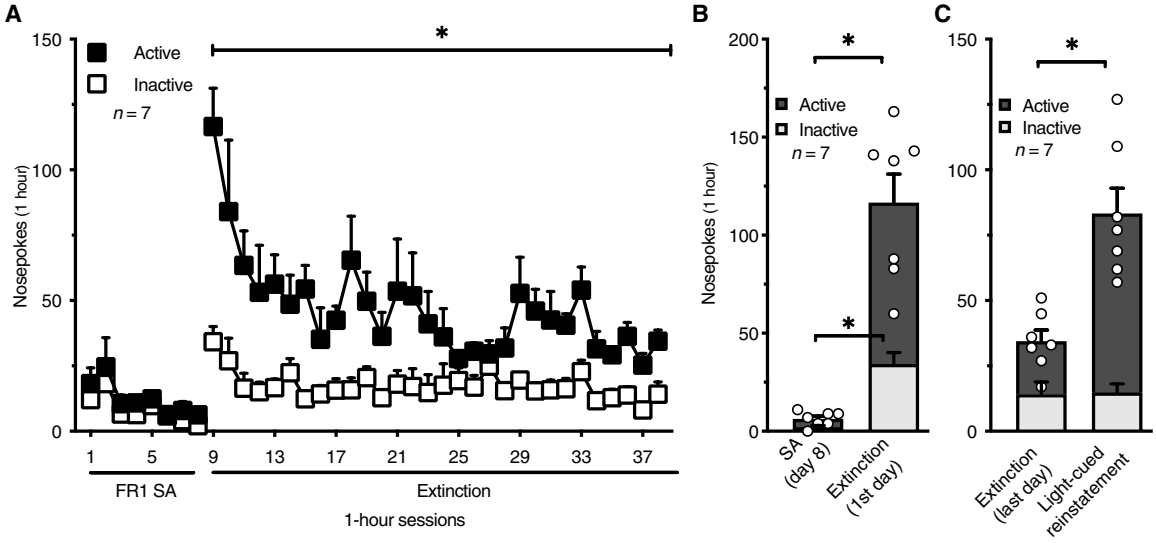

Fig. 3. Mice extinguish and reinstate fentanyl vapor seeking. (**A**) After 8 days of fentanyl vapor self-administration sessions, mice underwent extinction training in the absence of cues for 30 sessions. The number of active NP decreased over sessions, reflecting the extinction of drug seeking. Two-way RM ANOVA shows a significant sessions × NP interaction ($F_{29,348} = 2.23$; $P = 0.0004$) and significant effect of session on the number of NP ($F_{3.24,38.84} = 4.70$; $P = 0.006$). (**B**) The number of active NP increased significantly on day 1 of extinction training compared with the last day of fentanyl self-administration. Two-way RM ANOVA shows a significant training days × NP interaction ($F_{1,12} = 25.92$; $P = 0.0003$), indicating that day 1 of extinction affected active and inactive NP differently. (**C**) Mice showed robust light cue–induced reinstatement. Two-way RM ANOVA shows a significant reinstatement × NP interaction ($F_{1,12} = 17.44$; $P = 0.001$). SA, self-administration; *n*, number of mice. The data are expressed as means ± SEM. *$P < 0.05$.

and (iii) long-access fentanyl (LgA-Fen) group (n = 16, F/M = 8/8) that self-administered fentanyl vapor in 1-hour sessions (eight sessions), followed by 12-hour sessions (10 sessions, every other day; Fig. 4A). Mice in the LgA-Fen group escalated their fentanyl vapor self-administration across sessions, whereas no escalation was observed in the ShA-Fen or LgA-Veh group (Fig. 4A). These findings are consistent with sufentanil vapor self-administration in rats (*14*) and intravenous rat and mouse self-administration models (*9*, *17*, *18*). Linear regression indicated that the escalation slope in the LgA-Fen group [a = 4.0, confidence interval (CI): 2.5 to 5.6] was significantly greater than 0, unlike in the ShA-Fen and LgA-Veh groups, and all of the slopes in the three groups were different from each other (Fig. 4A). The number of vapor deliveries during the first hour of self-administration (Fig. 4B) in the LgA-Fen group also escalated. Both sexes exhibited significant escalation over time, but the escalation slope was significantly higher in male mice (fig. S6), suggesting that male and female mice escalated their intake at different rates. This finding may be related to the higher drug intake in females early during the escalation phase (fig. S7).

Naloxone-precipitated withdrawal

We tested somatic signs of naloxone-precipitated opioid withdrawal in mice from the escalation experiment after the last self-administration session. LgA-Fen mice exhibited significantly higher withdrawal scores compared with ShA-Fen mice, whereas LgA-Fen and ShA-Fen mice exhibited higher scores than LgA-Veh mice (fig. S8A). Female mice exhibited greater somatic withdrawal scores compared with male mice, and this difference was most pronounced in the ShA-Fen group (fig. S8B), consistent with intravenous heroin self-administration in mice (*9*). Similar sex differences were observed in humans with opioid use disorder, in which women presented more signs of opioid withdrawal as measured by the Clinical Opiate Withdrawal Scale (*19*).

Self-administration of capsaicin-adulterated fentanyl vapor

To test whether the mice continue to self-administer fentanyl vapor despite punishment, we added the respiratory irritant capsaicin (0.2%) to the fentanyl solution. LgA-Fen and LgA-Veh mice from the escalation cohort were gradually transitioned to 1-hour self-administration sessions over 5 days. This was followed by two sessions, in which fentanyl (or vehicle) was adulterated with capsaicin. Mice responded differently to capsaicin, depending on their history of fentanyl self-administration. LgA-Veh mice were the most susceptible to the suppressive effect of capsaicin on self-administration, whereas LgA-Fen mice were the most resistant (Fig. 5A). LgA-Veh mice exhibited a lower number of vapor deliveries on the first day of capsaicin exposure, whereas ShA-Fen and LgA-Fen mice did not. Although capsaicin reduced the number of vapor deliveries in the second session in both ShA-Fen and LgA-Fen mice, this effect was smaller in LgA-Fen mice (Fig. 5B). In the LgA-Fen group, 8 of 16 mice exhibited a <25% reduction of vapor deliveries in the second capsaicin session versus 3 of 16 mice in the ShA-Fen group. Only 1 of 16 mice in the LgA-Fen group exhibited a >75% reduction of vapor deliveries compared with 8 of 16 in the ShA-Fen group (Fig. 5B). Overall, these findings suggest that mice in the LgA-Fen group were more resistant to punishment than ShA-Fen mice, and both fentanyl groups were more resistant than LgA-Veh mice.

Effects of fentanyl vapor self-administration on $GABA_B$ receptor–mediated currents in VTA dopamine neurons

The activation of $GABA_B$ receptors on dopamine neurons causes a large hyperpolarization through the activation of G protein–coupled inwardly rectifying potassium (GIRK) channels (*20*) and results in a reduction of dopamine neuronal firing and dopamine release in several brain areas, including the striatum (*21*–*23*). Clinical and preclinical studies showed that striatal dopamine release in response to drugs or drug cues changes after chronic exposure to opioids (*24*–*26*). In addition, $GABA_B$ receptor currents in VTA dopamine neurons are known to be lower during acute and subacute (≤7 days) withdrawal after repeated, passive opioid administration (*27*, *28*).

To further validate our model of opioid self-administration, we investigated $GABA_B$ receptor–mediated currents in VTA dopamine neurons after 10 weeks of fentanyl self-administration, followed by

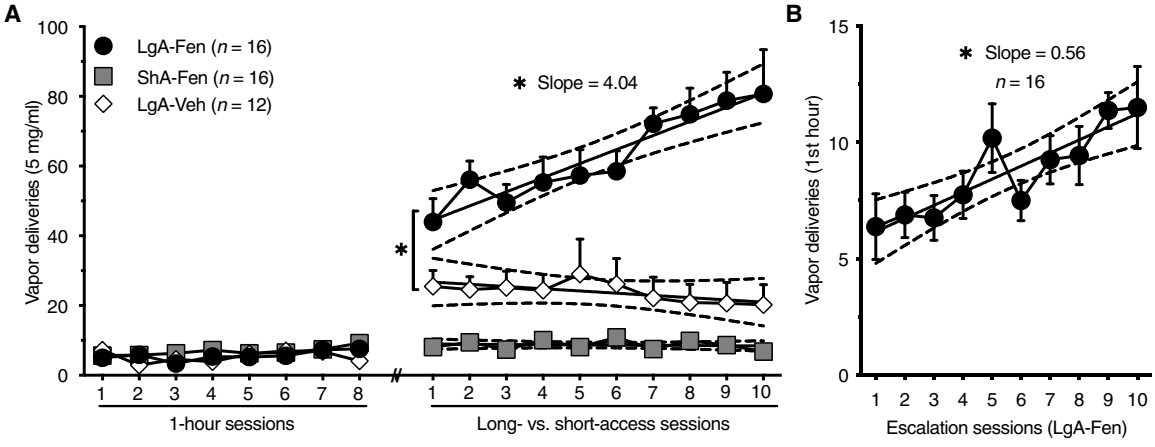

Fig. 4. Mice escalate fentanyl vapor self-administration. (**A**) The long-access fentanyl (LgA-Fen) group escalated their intake over time. Linear regression analysis shows a positive slope for the LgA-Fen group (a = 4.04; CI, 2.46 to 5.62), which is significantly greater than 0 ($F_{1,158}$ = 25.53; r^2 = 0.14; P < 0.0001). The calculated slopes for the short-access fentanyl (ShA-Fen) group (a = −0.058; CI, −0.33 to 0.22) and long-access vehicle (LgA-Veh) group (a = −0.64; CI, −1.92 to 0.63) were not different from 0. The slopes from the three groups were different from each other (test of equal slopes; $F_{2,434}$ = 18.77; P < 0.0001). (**B**) In the LgA-Fen group, the number of VD during the first hour of self-administration increased across escalation days (slope a = 0.56; CI, 0.31 to 0.82; $F_{1,158}$ = 18.82; r^2 = 0.11; P < 0.0001). *n,* number of mice. The data are expressed as means ± SEM. *P < 0.05.

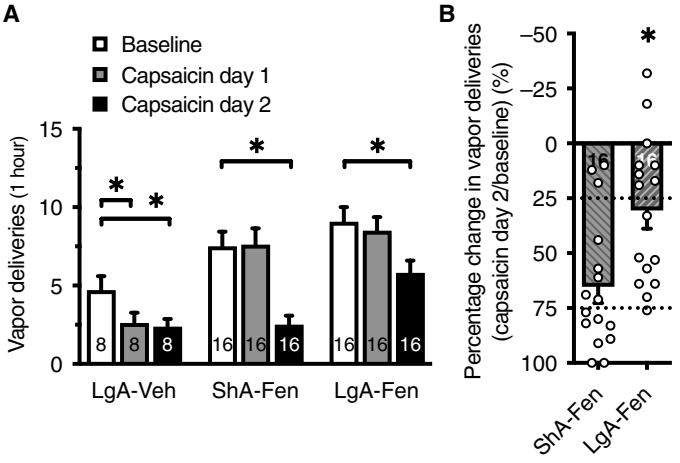

Fig. 5. Mice with a history of LgA-Fen vapor self-administration are more resistant to capsaicin-adulterated fentanyl. (**A**) The LgA-Veh group was most susceptible to the suppressive effects of capsaicin vapor, whereas the LgA-Fen group was the most resistant. Two-way RM ANOVA shows a significant capsaicin exposure × group interaction ($F_{4,74} = 3.01$; $P = 0.02$) and a significant effect of capsaicin on the number of VD ($F_{1.98,73.14} = 21.77$; $P < 0.0001$). The number of VD decreased only in the second capsaicin session in the ShA-Fen group ($P < 0.0001$) and LgA-Fen group ($P = 0.01$) of mice with a greater reduction in the ShA-Fen group compared with the LgA-Fen group. (**B**) Data from the second capsaicin session in ShA-Fen and LgA-Fen mice in (A) were normalized to baseline VD to illustrate the greater reduction of VD in the ShA-Fen group compared with the LgA-Fen group in response to the second capsaicin session (unpaired *t* test; $t_{30} = 3.13$; $P = 0.004$). Half of the LgA-Fen mice exhibited less than a 25% reduction of the number of VD, whereas half of the ShA-Fen mice exhibited greater than a 75% reduction. Dotted lines represent the quartiles. The number of mice (*n*) is shown in the bars. The data are expressed as means ± SEM. *$P < 0.05$.

4 weeks of abstinence. A cohort of mice that self-administered vaporized vehicle ($n = 5$ females) or fentanyl (5 mg/ml; $n = 5$ females) in 1-hour sessions (546 ± 35 vapor deliveries over 68 sessions) underwent forced abstinence for 1 month. Horizontal midbrain slices were prepared, and whole-cell voltage-clamp recordings from VTA dopamine neurons were performed. No significant differences in the membrane capacitance, input resistance, or magnitude of hyperpolarization-activated inward currents (I_h; measured at −138 mV) of dopamine neurons were found between the vehicle and fentanyl self-administration mice (fig. S9, A to C). In the presence of ionotropic glutamate receptor antagonists, $GABA_A$ receptor antagonist, and D_2 receptor antagonist, $GABA_B$ inhibitory postsynaptic currents (IPSCs) were evoked using a single stimulus or a train of electrical stimuli (3, 5, 7, or 9 at 60 Hz; Fig. 6, A to E). The amplitude of $GABA_B$ receptor IPSCs was lower in dopamine neurons in fentanyl self-administration mice compared with vehicle self-administration mice (Fig. 6, A to C). The average time to peak of IPSCs, which were measured from the time of the first stimulus, were 82 ± 3, 106 ± 3, 129 ± 3, 161 ± 2, and 194 ± 3 ms for one, three, five, seven, and nine stimuli, respectively, which is consistent with previous reports of $GABA_B$ receptor IPSCs in the VTA (*29*). The time to peak was not different between the vehicle and fentanyl groups. The stimulation intensity that was required to evoke a $GABA_B$ IPSC (with one stimulus) that was detectable over baseline noise was higher in slices from fentanyl self-administration mice compared with slices from vehicle self-administration mice (fig. S10). When normalized for the difference in stimulation intensity, the amplitude of $GABA_B$ receptor IPSCs in dopamine neurons from fentanyl self-administration mice was further reduced relative to vehicle self-administration mice (Fig. 6C). We next examined whether the lower $GABA_B$ receptor IPSC amplitude was attributable to presynaptic or postsynaptic changes. To test for the depression or facilitation of GABA release, we compared $GABA_B$ receptor IPSCs that were produced by a single stimulus with $GABA_B$ receptor IPSCs that were produced by trains of stimuli (*30*). In neurons from vehicle self-administration mice, a single stimulus produced $GABA_B$ IPSCs of 7.0 ± 0.4 pA, and nine stimuli produced $GABA_B$ receptor IPSCs of 46.7 ± 3.7 pA, whereas the arithmetic sum of nine individual IPSCs (1 stimulus × 9) was 52.5 ± 2.4 pA. The ratio (9 stimuli/[1 stimulus × 9]) was 0.88 ± 0.07, indicating paired-pulse depression and a higher probability of release (Fig. 6, D and E). In the fentanyl self-administration group, a single stimulus produced $GABA_B$ receptor IPSCs of 5.1 ± 0.4 pA, and nine stimuli produced $GABA_B$ receptor IPSCs of 39.3 ± 4.1 pA, whereas the arithmetic sum of nine individual IPSCs (1 stimulus × 9) was 32.7 ± 2.4 pA. The ratio (9 stimuli/[1 stimulus × 9]) was 1.2 ± 0.1, indicating paired-pulse facilitation and a lower probability of release (Fig. 6, D and E). Similarly, this ratio was calculated for three, five, and seven stimulus trains (Fig. 6E). Overall, these data indicated the lower probability of GABA release at $GABA_B$ synapses on VTA dopamine neurons following fentanyl self-administration and 4 weeks of protracted abstinence.

To investigate postsynaptic changes in $GABA_B$-GIRK signaling, we generated concentration-response curves in response to application of the $GABA_B$ receptor agonist (R)-baclofen. The data were fit with a sigmoid function with a Hill coefficient of 1. The half-maximally effective concentrations (EC_{50}) were consistent with expected values (*31*) and were not different between vehicle self-administration mice (1.87 μM) and fentanyl self-administration mice (1.77 μM). However, the maximal outward currents that were produced by (R)-baclofen were significantly smaller in neurons from fentanyl self-administration mice compared with vehicle self-administration mice (Fig. 6, F and G). Thus, the depression of $GABA_B$ receptor IPSCs following fentanyl self-administration was likely attributable to both pre- and postsynaptic neuroadaptations. The $GABA_B$ receptor IPSCs and responses to (R)-baclofen in vehicle self-administration mice were comparable to naïve mice, suggesting that lower $GABA_B$ receptor currents were specific to a history of fentanyl self-administration.

DISCUSSION

We developed and validated a noninvasive mouse model of opioid reinforcement using vaporized fentanyl self-administration, which recapitulates many core features of opioid use disorder in humans. We determined the effective concentration range of vaporized fentanyl to induce analgesia and motor activation and determined the resulting blood fentanyl levels. Blood fentanyl levels were consistent with the clinical literature in humans, in which the estimated serum concentrations for analgesia and anesthesia are 1 to 2 ng/ml and 10 to 20 ng/ml, respectively (*32*). We then found that mice self-administered fentanyl vapor, titrated their intake in response to different vaporized fentanyl concentrations and reinforcement schedules, and reinstated drug seeking after extinction in response to drug-associated cues. When given extended access to fentanyl, the mice escalated their drug intake, exhibited greater somatic signs of opioid withdrawal, and exhibited greater persistence in drug taking despite punishment, an index of compulsive-like behavior. Last, we showed that several weeks of limited access to fentanyl self-administration (1 hour/day)

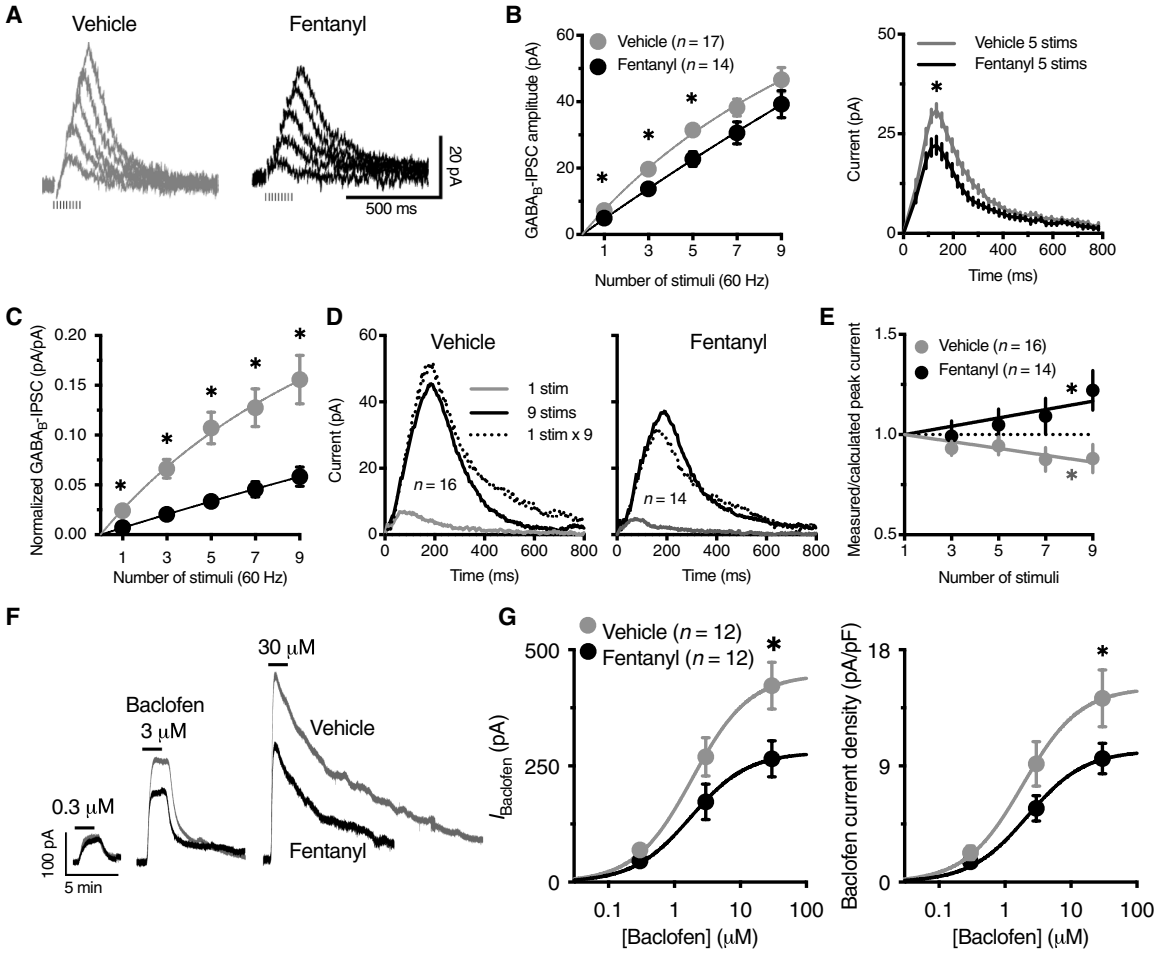

Fig. 6. Fentanyl vapor self-administration reduces $GABA_B$ receptor currents in VTA dopamine neurons through pre- and postsynaptic mechanisms. (**A**) Representative traces of $GABA_B$ IPSCs evoked by one, three, five, seven, or nine electrical stimuli (60 Hz) in slices from mice with a history of short access to vehicle versus fentanyl self-administration. Stimulus artifacts were blanked for clarity. (**B**) The amplitude of $GABA_B$ IPSCs was reduced in neurons from fentanyl versus vehicle mice, shown as the peak amplitude for one, three, five, seven, or nine stimuli (left; two-way RM ANOVA; $F_{1,29} = 5.44$; $P = 0.027$) and full time course for IPSCs evoked by five stimuli (right) (vehicle area under the curve = 6454, CI: 6117 to 6791; fentanyl area under the curve = 4709, CI: 4476 to 4942). (**C**) The plot of $GABA_B$ IPSC amplitudes that were normalized to the intensity of electrical stimulation shows a greater difference between vehicle and fentanyl $GABA_B$ IPSCs (stimulus × treatment interaction $F_{4,116} = 9.12$; $P < 0.0001$). (**D**) Representative traces of the arithmetically summed $GABA_B$ IPSCs (1 stimulus × 9) versus measured $GABA_B$ IPSC that were evoked by nine stimuli (9 stims) in slices from vehicle mice (left) (measured < calculated), suggesting paired-pulse depression, and fentanyl mice, (right) (measured > calculated), suggesting paired-pulse facilitation. (**E**) Ratio of the measured $GABA_B$-IPSC amplitude over the calculated amplitude for each number of stimuli. Linear regression shows a significantly negative slope for vehicle ($a = -0.02$; $F_{1,63} = 12.3$; $P = 0.0008$) and a significantly positive slope for fentanyl ($a = 0.021$; $F_{1,55} = 7.282$; $P = 0.009$). (**F**) Representative traces of whole-cell voltage-clamp recordings (baselined and peak-aligned) from vehicle versus fentanyl mice, demonstrating the concentration-dependent outward current produced by the application of (R)-baclofen. (**G**) The maximal outward current that was produced by (R)-baclofen was reduced in neurons from fentanyl mice compared with vehicle mice (left). The data were analyzed by nonlinear regression (sigmoidal fit; vehicle, $E_{max} = 446.9$ pA; fentanyl, $E_{max} = 279.6$ pA; $F_{1,51} = 7.35$; $P = 0.009$). No change in the EC_{50} was observed (vehicle, $EC_{50} = 1.87$ μM; fentanyl, $EC_{50} = 1.77$ μM). When the amplitude of the outward current was normalized to membrane capacitance (current density, pA/pF), the response to (R)-baclofen was still lower in fentanyl neurons (right). Solid lines represent the sigmoidal fit of the data. *n*, number of cells. The data are expressed as means ± SEM. *$P < 0.05$.

caused neuroadaptations of $GABA_B$ receptor–mediated currents in VTA dopamine neurons that persisted long after the cessation of self-administration, thus replicating and further extending previous studies of opioids and dopamine neurotransmission (*27*, *28*).

The reinforcing effects of drugs depend on the kinetics of drug delivery and bioavailability. Faster delivery of the same drug dose to the systemic circulation and central nervous system causes greater reinforcing effects (*33*, *34*). Inhaled drugs are rapidly absorbed by the extensive lung capillary bed into the left-side arterial circulation, whereas intravenous drugs are usually delivered to the right-side circulation, which may result in a ~35-s lag as suggested by models that compared inhaled versus intravenous morphine delivery (*11*). Thus, the inhalation route is hypothesized to be more reinforcing than the intravenous route by producing a faster onset of drug effect even when the resulting plasma concentration is equivalent (*34*, *35*).

Passive drug delivery through inhalation in rodent models of substance use disorder was initially pioneered with alcohol (*36*, *37*). Since then, operant models of alcohol vapor self-administration have been developed including in mice (*38*). Operant models of sufentanil-aerosol self-administration through inhalation using

nebulizer-based systems have also been described but remained of limited utility (*39*). However, the advent of the vaporizing technology used in e-cigarettes allowed the more precise and efficient vaporization of various substances, which facilitated the development of self-administration models of vaporized drugs (e.g., opioids and cannabis) in rats (*14*, *40*, *41*). No such models for non-alcohol substances have been reported in mice thus far.

The consistency of our data with the clinical and preclinical literature demonstrates the validity and feasibility of this model to study the neurobiology of drug reinforcement and different aspects of drug addiction, including the acquisition of drug self-administration, maintenance of drug intake, escalation and tolerance, compulsive drug seeking, extinction, abstinence, and the reinstatement of drug seeking. Overall, the utility of this mouse model is not limited to opioid addiction but could be extended to study other drugs of abuse.

This model could also be used to study the effects of the inhalation of different vehicle substances (i.e., non-drugs) on pulmonary function, and the abuse potential of novel systemic or central nervous system drugs (e.g., new drugs that are developed for the treatment of depression such as esketamine). The present model is useful for longitudinal studies with multiple episodes of drug self-administration and withdrawal throughout the natural life span of a species. For example, this model can be used to study the impact of drug self-administration during early adolescence on subsequent cognitive and emotional development and the vulnerability to drug use later in life. The vapor model is also compatible with techniques that require a tether (e.g., in vivo electrophysiology, optogenetics, calcium imaging, and microdialysis) and with concurrent self-administration of two or more different drugs. We are unaware of such studies in intravenous self-administration models in mice.

Although our data demonstrate volitional fentanyl vapor self-administration, the operant responding for non-drug cues was comparable to operant responding for fentanyl vapor on FR1 schedule during short-access (1 hour) sessions (Fig. 4 and fig. S4). This was similarly reported in intravenous self-administration models in mice and can ostensibly ascribe operant behavior for non-drug stimuli to volitional drug self-administration (*16*, *42*, *43*). Therefore, changing the drug concentration (Fig. 2, A and B), increasing the schedule of reinforcement (e.g., FR5 and FR10; Fig. 2, C and D), and using longer-access self-administration sessions (e.g., 12 hours; Fig. 4) can be used to ensure volitional drug self-administration. Other potential strategies include using variable-ratio schedules of reinforcement (*44*) and extinction of cues followed by reexposure to drugs (*16*).

Previous studies have shown that passive exposure to opioids reduces $GABA_B$ receptor–mediated currents in VTA dopamine neurons during early withdrawal (≤7 days) (*27*, *28*). In the present study, this effect persisted for at least 4 weeks after the last opioid self-administration session, which was likely caused by both pre- and postsynaptic mechanisms. The presynaptic mechanism has been previously demonstrated and attributed to an increase in adenosine tone that reduces GABA release at $GABA_B$ receptor–containing synapses (*27*, *28*). However, the postsynaptic mechanism remains largely unexplored.

A decrease in $GABA_B$ receptor–mediated currents in VTA dopamine neurons could suggest an increase in dopamine release from the disinhibition of these neurons upon activation. An opioid challenge results in greater mesolimbic dopamine release and dopamine cell firing in opioid-dependent animals compared with opioid-naïve animals (*26*, *45*, *46*). Furthermore, $GABA_B$ receptor agonism by direct agonists or positive allosteric modulators in the VTA blocks dopamine release in response to drugs (*22*, *23*), reduces the reinforcing properties of drugs, and inhibits the reinstatement of drug seeking in models of opioids and other drugs of abuse (*47*).

Notably, an extensive literature shows that VTA dopamine neuron firing and basal dopamine release are reduced shortly after the last exposure to opioids or upon precipitated withdrawal (*25*, *45*, *48*). However, these effects are observed in dependent animals, and basal dopamine release and VTA dopamine neuron firing recover to normal levels during subacute (≤7 days) and chronic withdrawal (≥14 days) (*25*, *45*). Consistent with these preclinical results is a positron emission tomography imaging study of abstinent opioid-dependent human subjects that showed higher striatal dopamine release after cue exposure, together with decreased D_2 receptor binding and anhedonia (*24*), indicating that anhedonia and greater craving can coexist in opioid addiction.

In conclusion, the versatility and noninvasiveness of this model in which male and female mice can self-administer drugs for extended periods of time and develop addiction-like behaviors, combined with myriad genetic tools and transgenic mouse lines, will permit investigation of the neurobiology of drug addiction in unprecedented ways, not possible with currently available models.

MATERIALS AND METHODS

Subjects

All of the experimental procedures were conducted in accordance with the guidelines of the National Institutes of Health (NIH) *Guide for the Care and Use of Laboratory Animals* and we with isoflurane (Henry Schein Animal Health re approved by the National Institute on Drug Abuse, Intramural Research Program, Animal Care and Use Committee. Male and female adult C57BL/6 mice (>10 weeks old) were obtained from The Jackson Laboratory (Bar Harbor, ME, USA). The studies were not designed to directly investigate sex differences, but mice of both sexes were included. Mice were housed two to four per cage and maintained under a 12-hour/12-hour light/dark cycle at 21 ± 2°C. All experiments were conducted during the dark cycle. Food and water were freely available in the home cages, and no food or water restriction was used to establish operant responding.

Apparatus

Operant vapor self-administration was conducted in eight airtight chambers (14 cm × 20 cm × 23 cm; La Jolla Alcohol Research, La Jolla, CA, USA; fig. S1) that were placed inside a black Plexiglas enclosure to minimize noise and light. Two nosepoke holes were mounted opposite to each other on the side walls. White light bulbs were mounted above the nosepoke holes. A vacuum pump maintained constant ambient airflow in the chambers. The outflowing air was filtered by an inline HEPA-Cap disposable filter and then disposed through the facility's exhaust system. To vaporize the drug, we used a vaporizing tank that was equipped with an atomizer (SMOK TFV8 X-Baby Tank; Shenzhen IVPS Technology, Shenzhen, China), which was filled with fentanyl or vehicle solutions. The atomizer was activated by an SVS250 vaporizer (Scientific Vapor, OR, USA). We used Med Associates software and interface (St. Albans, VT, USA) to record nosepokes and control activation of the vaporizers and light cue presentation. The suction system allowed the flow of vaporized drug into the operant chamber when the vaporizer was activated. The duration of drug vapor in the chamber depends on airflow rate, power setting of the

vaporizer, and vaporizing time. In our experiments, these were adjusted to allow drug clearance within 1 min after each vapor delivery (verified by visual inspection). In most of the experiments, we used an airflow rate of 1 to 2 liters/min, a power of 60 W, and a vaporizing duration of 1.5 s.

Self-administration

One nosepoke hole was active (i.e., resulting in vapor delivery and/or light cue presentation), and the other nosepoke hole was inactive (i.e., no scheduled consequences). Active nosepokes resulted in vapor delivery for ~1 min, which was associated with cue light presentation and a 1-min timeout period. All nosepokes were recorded throughout the entire session. The self-administration session durations were 1 or 12 hours, and these sessions were on FR1 schedule of reinforcement (i.e., each operant response on the active operandum resulted in a vapor delivery), except where specified. For vehicle self-administration, only vehicle vapor was delivered in response to active nosepokes (no fentanyl). For light cue "self-administration," only light was presented in response to active nosepokes (no vapor). Mice underwent five or six self-administration sessions per week (one session per day). The concentration of vaporized fentanyl was 0.1 to 30 mg/ml.

Extinction

Two cohorts of mice underwent extinction training after fentanyl self-administration. Some of the mice underwent extinction in the absence of the light cue and vehicle vapor (active nosepokes had no scheduled consequences; i.e., no fentanyl or vehicle vapor and no cues), and another group of mice underwent extinction training in the presence of vehicle vapor and light cue (only fentanyl was absent). Extinction sessions lasted 1 hour each, and the mice underwent 1 session per day for 30 sessions. One mouse was excluded retrospectively because it failed to extinguish self-administration behavior, defined as <60 active nosepokes over the last three extinction days.

Cue-induced reinstatement

An active nosepoke resulted in presentation of the light cue that was previously associated with fentanyl drug delivery, but no vapor was delivered.

Drugs

Fentanyl citrate (National Institute on Drug Abuse, Intramural Research Program Pharmacy, Baltimore, MD, USA) was added to 80% vegetable glycerol/20% propylene glycol. We dissolved fentanyl (0.1 to 30 mg/ml) by interleaved vortexing and sonication (~30 min in total) and then filtered the solution. The vaporized fentanyl concentration (in mg/ml) refers to the concentration of dissolved fentanyl that was used to fill the vaporizer tanks (not actual vapor concentration). Naloxone (1 mg/kg; Mylan Institutional Galway, Ireland) was dissolved in saline and injected intraperitoneally. Capsaicin (AK Scientific, Union City, CA, USA) was dissolved in 100% ethanol at 10 mg/ml and then mixed with fentanyl solution (5 mg/ml) for a final concentration of 0.2%. (R)-baclofen, picrotoxin, and NBQX (2,3-Dioxo-6-nitro-1,2,3,4-tetrahydrobenzo[*f*]quinoxaline-7-sulfonamide) were obtained from Tocris (Minneapolis, MN, USA). All of the other reagents for electrophysiology were obtained from Sigma-Aldrich (St. Louis, MO, USA).

Hot-plate test

A cohort of mice was passively exposed to fentanyl vapor (total of four vapor deliveries, evenly spaced over 8 min) to test the analgesic effects of fentanyl vapor. Fentanyl was dissolved at different concentrations (0 to 30 mg/ml) and delivered as vapor puffs. Mice were then placed on the hot plate (53.5°C; Ugo Basile) and observed for the latency of the presentation of signs of nociception (i.e., withdrawal/licking of hind paw, vocalization, or jumping). A 30-s cutoff was used to prevent tissue damage.

Locomotor test

Different cohorts of mice were used to measure the locomotor effects of different concentrations of fentanyl vapor. Mice were habituated to locomotor boxes (AccuScan Instruments, Columbus, OH, USA) for 2 days (1 hour/day). On the third day, mice were placed in the locomotor activity boxes for 30 min and then placed in the vapor chambers where they were passively exposed to fentanyl vapor (total of five vapor deliveries, evenly spaced over 10 min). Mice were then placed in the locomotor activity boxes for 1 hour to measure locomotion.

Blood fentanyl levels

Different cohorts of mice were passively exposed to different concentrations of fentanyl vapor (2.5 and 10 mg/ml; total of five vapor deliveries, evenly spaced over 60 min) to measure blood fentanyl levels. Two minutes after the last vapor delivery, mice were deeply anesthetized with isoflurane (Henry Schein Animal Health, Dublin, OH, USA) and 1 ml of blood was collected by cardiac puncture, placed in vacutainer ethylenediaminetetraacetic acid tubes, and frozen at −80°C. Blood fentanyl levels were analyzed by high-performance liquid chromatography/tandem mass spectrometry (NMS Labs, Willow Grove, PA, USA).

Escalation of fentanyl vapor self-administration

Mice were trained to self-administer fentanyl vapor (5 mg/ml) in eight 1-hour sessions on an FR1 schedule. This was followed by long-access (LgA) versus short-access (ShA) self-administration every other day for 10 sessions. The LgA mice were allowed to self-administer fentanyl vapor continuously for 12 hours. Consistent with previous studies (*9*, *49*) and based on pilot experiments in female mice that showed increased fentanyl vapor intake during the first 12-hour escalation session compared with male mice (fig. S7), female mice in the LgA-Fen group underwent three LgA sessions in which the number of vapor deliveries was capped before their escalation phase (two sessions capped at 30 vapor deliveries and one session capped at 60 vapor deliveries). Food and water were provided inside the operant chambers. The ShA mice did not have access to food during the 1-hour sessions. A control group was allowed to self-administer vehicle vapor (no fentanyl) in eight 1-hour sessions and then allowed to self-administer vehicle vapor in 12-hour sessions similarly to the LgA fentanyl group.

Naloxone-precipitated withdrawal

After the last self-administration session, mice from the escalation experiment (LgA-Veh, ShA-Fen, and LgA-Fen groups) received intraperitoneal naloxone (1 mg/kg). They were then placed in clear Plexiglas boxes (20 cm × 20 cm × 29 cm) and video-recorded for 20 min. The videos were scored by two observers (one of them blinded to experimental group) as previously described (*9*) to generate a total score of naloxone-precipitated somatic signs of withdrawal. Briefly, the withdrawal signs included jumps, paw tremor (clapping behavior), and wet dog shakes, which were weighted equally and given one

point for each occurrence. Mice were also observed for diarrhea, abnormal posture, salivation, and genital grooming, which were counted once per session. These points were added to yield the total withdrawal score. The scores from the two observers were averaged. The data are expressed as the total withdrawal score.

Capsaicin adulteration test

Capsaicin was added to the fentanyl or vehicle solutions [fentanyl (5 mg/ml), 0.2% capsaicin] and vaporized together with fentanyl or vehicle. Given the irritant properties of capsaicin, this allowed capsaicin vapor to serve as a punishment for fentanyl or vehicle vapor self-administration. After the naloxone-precipitated withdrawal experiment, ShA-Fen, LgA-Fen, and LgA-Veh mice from the escalation cohort continued to self-administer fentanyl or vehicle vapor for 3 days. The LgA-Fen and LgA-Veh mice were then gradually transitioned from 12-hour to 1-hour sessions over 5 days (one 6-hour session, one 3-hour session, and three 1-hour sessions). This was followed by two sessions in which fentanyl or vehicle solutions were adulterated with 0.2% capsaicin. This experimental paradigm allowed adequate comparisons between the different cohorts and avoided unequal capsaicin exposure per training session (1 hour versus 12 hours; pilot data showed an additive effect of capsaicin exposure). Data from the capsaicin sessions were compared with the pre-capsaicin number of vapor deliveries (3-day average).

Electrophysiological recordings

The mice were deeply anesthetized with isoflurane and euthanized by decapitation. Brains were quickly removed and placed in warm (30°C) modified Krebs buffer that contained 125 mM NaCl, 2.5 mM KCl, 1.2 mM $MgCl_2$, 2.4 mM $CaCl_2$, 1.25 mM NaH_2PO_4, 11 mM D-glucose, and 23.8 mM $NaHCO_3$, bubbled with 95% O_2/5% CO_2 with 5 μM MK-801 to reduce excitotoxicity and increase slice viability. In the same solution, horizontal midbrain slices (200 μm) that contained the VTA were obtained using a vibrating microtome (Leica Biosystems, Wetzlar, Germany), maintained at 32°C for 30 min, and then kept at room temperature until use. Dopamine neurons in the VTA were identified by their location medial to the medial terminal nucleus of the accessory optic tract, the presence of a slowly developing inward current (I_h > 100 pA) upon membrane hyperpolarization (1.5-s steps; V_{hold}: −68 to −138 mV, −10-mV increments), low firing frequency (<10 Hz) in cell-attached or whole-cell modes, and broad (>1.2 ms) action potentials (*50*, *51*). For I_h measurements, the instantaneous leak current that was produced by the voltage step was subtracted. Whole-cell patch-clamp recordings were obtained from neurons at 35 ± 1°C using MultiClamp 700B amplifiers (Molecular Devices, Sunnyvale, CA, USA) and Digidata 1440A digitizers (Molecular Devices) with Clampex and Axoscope software (Molecular Devices) in modified Krebs buffer (as above) with 3 μM NBQX, 100 μM picrotoxin, and 600 nM sulpiride to isolate $GABA_B$ receptor–mediated synaptic transmission. The pipette resistance was 1 to 3 megohms when filled with an internal solution that contained 122 mM K-methylsulfate, 10 mM Hepes, 0.45 mM EGTA, 9 mM NaCl, 1.8 mM $MgCl_2$, 0.1 mM $CaCl_2$, 4 mM Mg–adenosine triphosphate (ATP), 0.3 mM Na–guanosine triphosphate (GTP), and 14 mM creatine phosphate disodium (pH 7.35 and 283 mOsm). Cell capacitance for current density was determined by fitting the averaged capacitive transient (ΔV = 5 mV) with a double exponential and then using τ_{fast} and access resistance determined by Clampex for the same steps. (R)-baclofen was bath-applied. $GABA_B$ receptor–mediated IPSCs were evoked by electrical stimulation using a single stimulus or train of stimuli (three, five, seven, or nine stimuli at 60 Hz, 0.5 ms for each stimulus; V_{hold}, −68 mV). The reported voltages were corrected for a −8-mV liquid junction potential between the internal and external solutions. The IPSC peak amplitude represents the average of data points over 20 ms. Multiplicative IPSCs (e.g., 1 stimulus × 9) were determined by adding the current that was obtained by a single stimulus to itself while shifting the onset of each IPSC by ~17 ms to account for 60-Hz stimulation (*30*). Normalized measured/calculated peak currents were fit by linear regression. Concentration-response curves were analyzed by least-squares fit (constraints: bottom = 0, EC_{50} > 0; Hill coefficient = 1). The recordings were performed by two investigators, one of whom was always blinded to the experimental group (vehicle versus fentanyl vapor).

Statistical analysis

We used *t* tests (paired or unpaired) and analysis of variance [ANOVA; one- or two-way, with or without repeated measures (RM)] followed by Sidak's multiple-comparison post hoc test. We also analyzed some of the data using regression models, both linear (we ensured that there were no departures from linearity with replicates test) and nonlinear (sigmoidal fits). The details are presented in Results. Male versus female data were highlighted when sex differences were observed. We used Prism 8.1.1 software (GraphPad, San Diego, CA, USA) to graph and analyze the data. Statistical significance was set at $P \leq 0.05$. All data are expressed as means and SEM or means and 95% CIs.

SUPPLEMENTARY MATERIALS

Supplementary material for this article is available at http://advances.sciencemag.org/cgi/content/full/6/32/eabc0413/DC1

View/request a protocol for this paper from *Bio-protocol*.

REFERENCES AND NOTES

1. GBD 2016 Alcohol; Drug Use Collaborators, The global burden of disease attributable to alcohol and drug use in 195 countries and territories, 1990-2016: A systematic analysis for the Global Burden of Disease Study 2016. *Lancet Psychiatry* **5**, 987–1012 (2018).
2. S. Larney, L. T. Tran, J. Leung, T. Santo Jr., D. Santomauro, M. Hickman, A. Peacock, E. Stockings, L. Degenhardt, All-cause and cause-specific mortality among people using extramedical opioids: A systematic review and meta-analysis. *JAMA Psychiat.* **77**, 1–10 (2019).
3. C. M. Jones, E. B. Einstein, W. M. Compton, Changes in synthetic opioid involvement in drug overdose deaths in the United States, 2010-2016. *JAMA* **319**, 1819–1821 (2018).
4. K. Kuczyńska, P. Grzonkowski, Ł. Kacprzak, J. B. Zawilska, Abuse of fentanyl: An emerging problem to face. *Forensic Sci. Int.* **289**, 207–214 (2018).
5. A. Belin-Rauscent, M. Fouyssac, A. Bonci, D. Belin, How preclinical models evolved to resemble the diagnostic criteria of drug addiction. *Biol. Psychiatry* **79**, 39–46 (2016).
6. D. J. Reiner, I. Fredriksson, O. M. Lofaro, J. M. Bossert, Y. Shaham, Relapse to opioid seeking in rat models: Behavior, pharmacology and circuits. *Neuropsychopharmacology* **44**, 465–477 (2019).
7. G. F. Koob, Neurobiology of opioid addiction: Opponent process, hyperkatifeia, and negative reinforcement. *Biol. Psychiatry* **87**, 44–53 (2020).
8. Y. Zhang, Y. Liang, M. Randesi, V. Yuferov, C. Zhao, M. J. Kreek, Chronic oxycodone self-administration altered reward-related genes in the ventral and dorsal striatum of C57BL/6J mice: An RNA-seq analysis. *Neuroscience* **393**, 333–349 (2018).
9. E. B. Towers, B. J. Tunstall, M. L. McCracken, L. F. Vendruscolo, G. F. Koob, Male and female mice develop escalation of heroin intake and dependence following extended access. *Neuropharmacology* **151**, 189–194 (2019).
10. D. T. Arena, H. E. Covington III, J. F. DeBold, K. A. Miczek, Persistent increase of I.V. cocaine self-administration in a subgroup of C57BL/6J male mice after social defeat stress. *Psychopharmacology* **236**, 2027–2037 (2019).
11. M. Dershwitz, J. L. Walsh, R. J. Morishige, P. M. Connors, R. M. Rubsamen, S. L. Shafer, C. E. Rosow, Pharmacokinetics and pharmacodynamics of inhaled versus intravenous morphine in healthy volunteers. *Anesthesiology* **93**, 619–628 (2000).

12. L. J. Vanderschuren, P. W. Kalivas, Alterations in dopaminergic and glutamatergic transmission in the induction and expression of behavioral sensitization: A critical review of preclinical studies. *Psychopharmacology* **151**, 99–120 (2000).
13. C. D. Bryant, K. W. Roberts, C. S. Culbertson, A. Le, C. J. Evans, M. S. Fanselow, Pavlovian conditioning of multiple opioid-like responses in mice. *Drug Alcohol Depend.* **103**, 74–83 (2009).
14. J. C. M. Vendruscolo, B. J. Tunstall, S. A. Carmack, B. E. Schmeichel, E. G. Lowery-Gionta, M. Cole, O. George, S. A. Vandewater, M. A. Taffe, G. F. Koob, L. F. Vendruscolo, Compulsive-like sufentanil vapor self-administration in rats. *Neuropsychopharmacology* **43**, 801–809 (2018).
15. S. A. Carmack, R. J. Keeley, J. C. M. Vendruscolo, E. G. Lowery-Gionta, H. Lu, G. F. Koob, E. A. Stein, L. F. Vendruscolo, Heroin addiction engages negative emotional learning brain circuits in rats. *J. Clin. Invest.* **129**, 2480–2484 (2019).
16. M. Thomsen, S. B. Caine, False positive in the intravenous drug self-administration test in C57BL/6J mice. *Behav. Pharmacol.* **22**, 239–247 (2011).
17. Y. Zhang, B. Mayer-Blackwell, S. D. Schlussman, M. Randesi, E. R. Butelman, A. Ho, J. Ott, M. J. Kreek, Extended access oxycodone self-administration and neurotransmitter receptor gene expression in the dorsal striatum of adult C57BL/6 J mice. *Psychopharmacology* **231**, 1277–1287 (2014).
18. S. H. Ahmed, J. R. Walker, G. F. Koob, Persistent increase in the motivation to take heroin in rats with a history of drug escalation. *Neuropsychopharmacology* **22**, 413–421 (2000).
19. S. E. Back, R. L. Payne, A. H. Wahlquist, R. E. Carter, Z. Stroud, L. Haynes, M. Hillhouse, K. T. Brady, W. Ling, Comparative profiles of men and women with opioid dependence: Results from a national multisite effectiveness trial. *Am. J. Drug Alcohol Abuse* **37**, 313–323 (2011).
20. S. W. Johnson, R. A. North, Two types of neurone in the rat ventral tegmental area and their synaptic inputs. *J. Physiol.* **450**, 455–468 (1992).
21. S. Erhardt, J. M. Mathé, K. Chergui, G. Engberg, T. H. Svensson, $GABA_B$ receptor-mediated modulation of the firing pattern of ventral tegmental area dopamine neurons in vivo. *Naunyn Schmiedebergs Arch. Pharmacol.* **365**, 173–180 (2002).
22. P. W. Kalivas, P. Duffy, H. Eberhardt, Modulation of A10 dopamine neurons by gamma-aminobutyric acid agonists. *J. Pharmacol. Exp. Ther.* **253**, 858–866 (1990).
23. Z. X. Xi, E. A. Stein, Baclofen inhibits heroin self-administration behavior and mesolimbic dopamine release. *J. Pharmacol. Exp. Ther.* **290**, 1369–1374 (1999).
24. F. Zijlstra, J. Booij, W. van den Brink, I. H. A. Franken, Striatal dopamine D_2 receptor binding and dopamine release during cue-elicited craving in recently abstinent opiate-dependent males. *Eur. Neuropsychopharmacol.* **18**, 262–270 (2008).
25. E. Acquas, G. Di Chiara, Depression of mesolimbic dopamine transmission and sensitization to morphine during opiate abstinence. *J. Neurochem.* **58**, 1620–1625 (1992).
26. D. W. Johnson, S. D. Glick, Dopamine release and metabolism in nucleus accumbens and striatum of morphine-tolerant and nontolerant rats. *Pharmacol. Biochem. Behav.* **46**, 341–347 (1993).
27. A. Bonci, J. T. Williams, A common mechanism mediates long-term changes in synaptic transmission after chronic cocaine and morphine. *Neuron* **16**, 631–639 (1996).
28. Y. Shoji, J. Delfs, J. T. Williams, Presynaptic inhibition of $GABA_B$-mediated synaptic potentials in the ventral tegmental area during morphine withdrawal. *J. Neurosci.* **19**, 2347–2355 (1999).
29. C. D. Fiorillo, J. T. Williams, Glutamate mediates an inhibitory postsynaptic potential in dopamine neurons. *Nature* **394**, 78–82 (1998).
30. M. J. Beckstead, C. P. Ford, P. E. M. Phillips, J. T. Williams, Presynaptic regulation of dendrodendritic dopamine transmission. *Eur. J. Neurosci.* **26**, 1479–1488 (2007).
31. M. G. Lacey, N. B. Mercuri, R. A. North, On the potassium conductance increase activated by GABAB and dopamine D2 receptors in rat substantia nigra neurones. *J. Physiol.* **401**, 437–453 (1988).
32. European Monitoring Centre for Drugs and Drug Addiction, Fentanyl drug profile (2015); https://www.emcdda.europa.eu/publications/drug-profiles/fentanyl.
33. L. A. Marsch, W. K. Bickel, G. J. Badger, J. P. Rathmell, M. D. Swedberg, B. Jonzon, C. Norsten-Höög, Effects of infusion rate of intravenously administered morphine on physiological, psychomotor, and self-reported measures in humans. *J. Pharmacol. Exp. Ther.* **299**, 1056–1065 (2001).
34. N. D. Volkow, G. J. Wang, M. W. Fischman, R. Foltin, J. S. Fowler, D. Franceschi, M. Franceschi, J. Logan, S. J. Gatley, C. Wong, Y. S. Ding, R. Hitzemann, N. Pappas, Effects of route of administration on cocaine induced dopamine transporter blockade in the human brain. *Life Sci.* **67**, 1507–1515 (2000).
35. R. W. Foltin, M. W. Fischman, Self-administration of cocaine by humans: Choice between smoked and intravenous cocaine. *J. Pharmacol. Exp. Ther.* **261**, 841–849 (1992).
36. D. B. Goldstein, N. Pal, Alcohol dependence produced in mice by inhalation of ethanol: Grading the withdrawal reaction. *Science* **172**, 288–290 (1971).
37. L. F. Vendruscolo, A. J. Roberts, Operant alcohol self-administration in dependent rats: Focus on the vapor model. *Alcohol* **48**, 277–286 (2014).
38. K. M. Kantak, C. Luzzo, Ethanol vapor self-administration in adult C57BL/6J male mice. *Drug Alcohol Depend.* **86**, 123–131 (2007).
39. A. B. Jaffe, L. G. Sharpe, J. H. Jaffe, Rats self-administer sufentanil in aerosol form. *Psychopharmacology* **99**, 289–293 (1989).
40. T. G. Freels, L. N. Baxter-Potter, J. M. Lugo, N. C. Glodosky, H. R. Wright, S. L. Baglot, G. N. Petrie, Z. Yu, B. H. Clowers, C. Cuttler, R. A. Fuchs, M. N. Hill, R. J. McLaughlin, Vaporized cannabis extracts have reinforcing properties and support conditioned drug-seeking behavior in rats. *J. Neurosci.* **40**, 1897–1908 (2020).
41. A. Gutierrez, J. D. Nguyen, K. M. Creehan, M. A. Taffe, Self-administration of heroin by vapor inhalation in female Wistar rats. bioRxiv 2020.03.30.016725 [**Preprint**]. 31 March 2020. https://doi.org/10.1101/2020.03.30.016725.
42. G. B. Kish, Learning when the onset of illumination is used as reinforcing stimulus. *J. Comp. Physiol. Psychol.* **48**, 261–264 (1955).
43. C. M. Olsen, D. G. Winder, Operant sensation seeking engages similar neural substrates to operant drug seeking in C57 mice. *Neuropsychopharmacology* **34**, 1685–1694 (2009).
44. A. J. López, A. R. Johnson, A. J. Kunnath, J. E. Zachry, K. C. Thibeault, M. G. Kutlu, C. A. Siciliano, E. S. Calipari, An optimized procedure for robust volitional drug intake in mice. bioRxiv 786616 [**Preprint**]. 30 September 2019. https://doi.org/10.1101/786616.
45. M. Diana, A. L. Muntoni, M. Pistis, M. Melis, G. L. Gessa, Lasting reduction in mesolimbic dopamine neuronal activity after morphine withdrawal. *Eur. J. Neurosci.* **11**, 1037–1041 (1999).
46. P. W. Kalivas, J. Stewart, Dopamine transmission in the initiation and expression of drug- and stress-induced sensitization of motor activity. *Brain Res. Brain Res. Rev.* **16**, 223–244 (1991).
47. M. Filip, M. Frankowska, GABAB receptors in drug addiction. *Pharmacol. Rep.* **60**, 755–770 (2008).
48. E. Pothos, P. Rada, G. P. Mark, B. G. Hoebel, Dopamine microdialysis in the nucleus accumbens during acute and chronic morphine, naloxone-precipitated withdrawal and clonidine treatment. *Brain Res.* **566**, 348–350 (1991).
49. J. B. Becker, G. F. Koob, Sex differences in animal models: Focus on addiction. *Pharmacol. Rev.* **68**, 242–263 (2016).
50. B. Chieng, Y. Azriel, S. Mohammadi, M. J. Christie, Distinct cellular properties of identified dopaminergic and GABAergic neurons in the mouse ventral tegmental area. *J. Physiol.* **589**, 3775–3787 (2011).
51. S. Lammel, D. I. Ion, J. Roeper, R. C. Malenka, Projection-specific modulation of dopamine neuron synapses by aversive and rewarding stimuli. *Neuron* **70**, 855–862 (2011).

Acknowledgments: We thank Y. Shaham for critical feedback and suggestions, M. Cole for technical assistance, and M. Arends for proofreading the manuscript. **Funding:** This project was supported by the Intramural Research Program at the National Institute on Drug Abuse (DA048530 to B.J.T. and DA048085 to K.M.). S.C.G. and R.C.N.M. were supported by a fellowship from the Center on Compulsive Behaviors at the NIH. **Author contributions:** K.M., M.M.O., S.C.G., B.J.T., R.C.N.M., G.F.K., and L.F.V. designed the experiments. K.M., M.M.O., and R.C.N.M. performed the behavioral experiments. K.M. and S.C.G. performed the electrophysiology experiments. K.M. prepared the figures. K.M., M.M.O., S.C.G., and L.F.V. analyzed the data. K.M., M.M.O., S.C.G., B.J.T., R.C.N.M., A.B., G.F.K., and L.F.V. wrote and edited the manuscript. **Competing interests:** The authors declare that they have no competing interests. The opinions expressed in this article are the authors' own and do not reflect the views of the NIH/DHHS. **Data and materials availability:** All data needed to evaluate the conclusions in the paper are present in the paper and/or the Supplementary Materials. Additional data related to this paper may be requested from the authors.

Submitted 2 April 2020
Accepted 17 June 2020
Published 5 August 2020
10.1126/sciadv.abc0413

Citation: K. Moussawi, M. M. Ortiz, S. C. Gantz, B. J. Tunstall, R. C. N. Marchette, A. Bonci, G. F. Koob, L. F. Vendruscolo, Fentanyl vapor self-administration model in mice to study opioid addiction. *Sci. Adv.* **6**, eabc0413 (2020).

Fentanyl vapor self-administration model in mice to study opioid addiction

K. Moussawi, M. M. Ortiz, S. C. Gantz, B. J. Tunstall, R. C. N. Marchette, A. Bonci, G. F. Koob and L. F. Vendruscolo

Sci Adv **6** (32), eabc0413.
DOI: 10.1126/sciadv.abc0413